Pergamon

Cement and Concrete Research 32 (2002) 97–101

CEMENT AND CONCRETE RESEARCH

Structure–texture correlation in ultra-high-performance concrete A nuclear magnetic resonance study

Charlotte Porteneuve[a,*], Jean-Pierre Korb[b], Dominique Petit[b], Hélène Zanni[a]

[a]*Laboratoire de Physique et Mécanique des Milieux Hétérogènes, UMR CNRS 7636, Ecole Supérieure de Physique et Chimie Industrielles, 10, rue Vauquelin, 75231 Paris Cedex 05, France*

[b]*Laboratoire de Physique de la Matière Condensée, UMR CNRS 7643, Ecole Polytechnique, 91128 Palaiseau, France*

Received 29 March 2000; accepted 25 July 2001

Abstract

The pore size distribution in three reactive powder concrete formulations has been studied by nuclear magnetic relaxation of protons. Confirming the discrete and fractal features of the distribution for this kind of concrete, each formulation is assessed a surface fractal dimension, which reveals the hierarchy of pores. The experimental results evidence a dependence between this dimension and both the filling ratio of cement grains and the reactivity of silica fume. ^{29}Si nuclear magnetic resonance (NMR) allows us to draw a relationship between the amount of calcium silicate hydrates (C-S-H) and this surface fractal dimension. © 2002 Elsevier Science Ltd. All rights reserved.

Keywords: High-performance concrete; Microstructure; Particle size distribution; Pore size distribution; Nuclear magnetic resonance

1. Introduction

The important mechanical and durable performances of reactive powder concrete are mainly due to the high compactness of this material made of sand, crushed quartz, cement, and silica fume. In addition to their chemical reactivity, the granular packing of the various dry components proposed by Richard and Cheyrezy [1] approaches the hierarchical Apollonian packing through a wise choice of the size grading of each component. This concrete still possesses microporous features, which may govern most of its permeability properties. Usual methods of investigation of porosity are mercury porosimetry, differential scanning calorimetry, and nitrogen sorption to a lesser extent. These methods are either invasive, give access to open porosity only, imply a deterioration of the sample or the use of very low temperatures. In the present work, we propose a nondestructive method, proton nuclear magnetic relaxation, in order to study three kinds of reactive powder concrete, which will then be compared to a more conventional concrete. This method, which can be performed at room temperature, is sensitive to both open and closed porosity in a wide range. Previous studies [2–4] also showed its relevance as far as the kinetics of hydration is concerned, and evidenced the hierarchical character of the pore sizes in reactive powder concrete. More specifically, we have studied in this paper the influence of the filling ratio of the cement grains and of the specific surface area of silica fume on the pore size distribution of three reactive powder concrete formulations. ^{29}Si nuclear magnetic resonance (NMR) is used to find a correlation with the amount of calcium silicate hydrates (C-S-H). As the porosity is quite sensitive to the granular packing, we worked on materials as close as possible to actual reactive powder concrete, except for the metallic fibers, which rule out NMR experiments.

2. Experimental

2.1. Materials

Three different reactive powder concrete specimens have been studied in the present work. As a basis for comparison, an ordinary concrete was also prepared. The specific characteristics of the concrete mixes are given in Table 1. The experiments were performed on one-month-old samples. They are composed of all the dry components actually

---

* Corresponding author. Tel.: +33-1-40-79-45-56; fax: +33-1-40-79-47-95.

E-mail address: charlie@pmmh.espci.fr (C. Porteneuve).

PII: S0008-8846(01)00635-4

Table 1
Characteristic of the concrete mixes; weight ratios in term of cement mass

Formulations		C_1 coefficient, silica fume S_1 (12 m^2/g BET)	C_2 coefficient, silica fume S_1 (12 m^2/g BET)	C_1 coefficient, silica fume S_2 (21.5m^2/g BET)	Ordinary concrete
Components	Granulometry				
Cement	$\phi = 15$ μm	1.000	1.000	1.000	1.000
Silica fume	$\phi = 0.5$ μm	0.325	0.150	0.325	–
Crushed quartz	$\phi = 5$ μm	0.300	0.150	0.300	–
Sand	$\phi = 330$ μm	1.430	2.000	1.430	–
Water	–	0.200	0.240	0.240	0.410
Siliceous agg.	ϕ up to 16 mm	–	–	–	4.585

The samples were mixed at 20 °C. The reactive powder concrete specimens only were then cured at 90 °C during 48 h after demolding. The filling ratios C_1 and C_2 are 2.2 and 1.1, respectively. The cement used is a low-alkali content cement with 22.7% SiO_2 and 4.3% Fe_2O_3. The experiments were performed on one-month-old specimens. The siliceous aggregates used in the ordinary concrete are of feltspatic/granitic origin.

present in real concrete, i.e., sand, crushed quartz, cement, and silica fume for reactive powder concrete, and cement and coarse aggregates for the ordinary concrete. The formers were formulated in order to emphasize two parameters: the type of silica fume and the filling ratio. The latter parameter is related to the compactness of cement grains and is equal to the ratio of the volume occupied by the fine particles in between the cement grains and the theoretical volume of the voids in a dense packing of cement grains. The filling ratio for each of the dry constituents can also be calculated. The higher it is, the higher is the silica fume content while the closer it is to one, the denser is the cement granular packing. The reactive powder concrete samples under investigation present two different filling ratios labeled C_1 and C_2, which are 2.2 and 1.1, respectively. The two silica fumes, labeled S_1 and S_2, differ by their BET surfaces: 12 and 21.5 m^2/g, respectively.

2.2. NMR experiments and processing method

We have performed a measurement of the longitudinal proton magnetization decay in the four concrete samples through the usual inversion recovery method at 300 MHz in static conditions on a Bruker ASX300 spectrometer at room temperature. Coarse pieces of concrete are used in order to limit the water adsorption on the surface of the grains. A representative example of the proton magnetization decay in reactive powder concrete is displayed in Fig. 1. As in previous experiments on similar materials [2–4], we observed a strongly nonexponential decay for all the samples. The application of several methods for processing this type of curve, including the Laplace inverse transformation [5], has evidenced the suitability of a weighted sum of five well-resolved single exponential functions to the fitting of the decay. The spreading of the respective relaxation times over five orders of magnitude and the average factor of 7.3 up to 9 between two consecutive times supports this decomposition. The frequency dependence of the measured proton relaxation times also observed in a previous study on reactive powder concrete [2] has validated the theoretical prediction in terms of a biphasic fast exchange model. The model implies nuclear relaxation of protons through hydrated paramagnetic ferric ions such as Fe^{3+} present at the surface of the pores and evidenced by ESR [3]. This process has drastic effects on the relaxation times and overwhelms the pure nuclear dipole–dipole relaxation expected in solids. The attribution of this relaxation times distribution to five different average pore sizes is then possible, assuming a spherical pore shape, and implies the following linear relation between the ith spin-lattice relaxation time $T_{1,i}$ and the ith average pore size $\langle R \rangle_i$ [3]:

$$\langle R \rangle_i = (30 N_s v_{\mathrm{solv}} H_I^2 n T_{1e}) T_{1,i}. \tag{1}$$

Here N_s is the surface density of paramagnetic spins, v_{solv} the volume of the solvation cage made by the paramagnetic impurity and the water molecules interacting with it, H_I the dipole–dipole coupling between the paramagnetic spin S (Fe^{3+} ions) and the proton spin I, n the average number of water molecules in the volume v_{solv}, and T_{1e} is the electron spin-lattice relaxation time of Fe^{3+} ions. All these parameters are known except for N_s, which can be found by an Electron Spin Resonance experiment. An important consequence of such a linear dependence is that the distribution of average pore radii $\langle R \rangle_i$ is similar to the one of relaxation times $T_{1,i}$.

The combination of various techniques for measuring the pore size distribution, such as mercury intrusion porosimetry, nitrogen and water sorption, also supports a porous

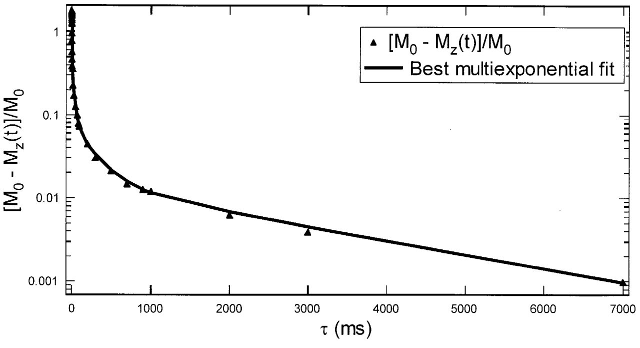

Fig. 1. Semilogarithmic plot of the recovery of proton magnetization at 300 MHz, at room temperature for the one-month-old reactive powder concrete with C_1 coefficient and silica fume S_2 (21.5 m^2/g).

structure decomposed into five modes in concrete [6]. The two largest porous modes are assessed to macroporosity, while the three smaller ones are relative to the C-S-H-induced porosity.

In complement, we have performed ^{29}Si NMR experiments on the same ground concrete samples. The Magic Angle Spinning (MAS) single pulse spectra have been obtained on an 11.7-Tesla Bruker ASX500 spectrometer with a cross-polarization CPMAS probe for 4-mm zirconium oxide rotors at 7 kHz.

3. Results and discussion

3.1. ^{1}H relaxation measurement

Basically, two pieces of information can be extracted from the magnetization decay displayed in Fig. 1: the different spin-lattice relaxation times $T_{1,i}$ and their respective prefactors $P_{1,i}$, which are the relative amount of protons expressed in percentage of the *i*th category of pores relaxing with $T_{1,i}$. The dependence of the fraction of protons with the measured relaxation rates $T_{1,i}$ for the four concrete formulations is displayed in Fig. 2. As $T_{1,i}$ is proportional to $\langle R\rangle_i$, the relation given in Eq. (1) allows us to express these results in terms of pore size. A similar behavior was observed for all three reactive powder concrete samples: we find a discrete distribution of $T_{1,i}$, which, except for the shortest, is reproducibly aligned in log–log scale. This evidences a power law over four orders of magnitude between the amount of protons and the average pore size. From a mathematical point of view, a power law is also expected in the computation of the total surface area $S_{\text{total}}(i)$ for each pore category $\langle R\rangle_i$ in a hierarchical distribution of noncommunicating or badly communicating spherical pores:

$$S_{\text{total}}(i) \propto \langle R\rangle_i^{2-D_f}, \tag{2}$$

where D_f is the fractal dimension of the surface. As $2 \leq D_f \leq 3$, Eq. (2) diverges in the range of the low radii. On the other hand, the expression of the total volume $V_{\text{total}}(i)$ as a function of $\langle R\rangle_i$ smoothly converges according to Eq. (3):

$$V_{\text{total}}(i) \propto \langle R\rangle_i^{3-D_f} \tag{3}$$

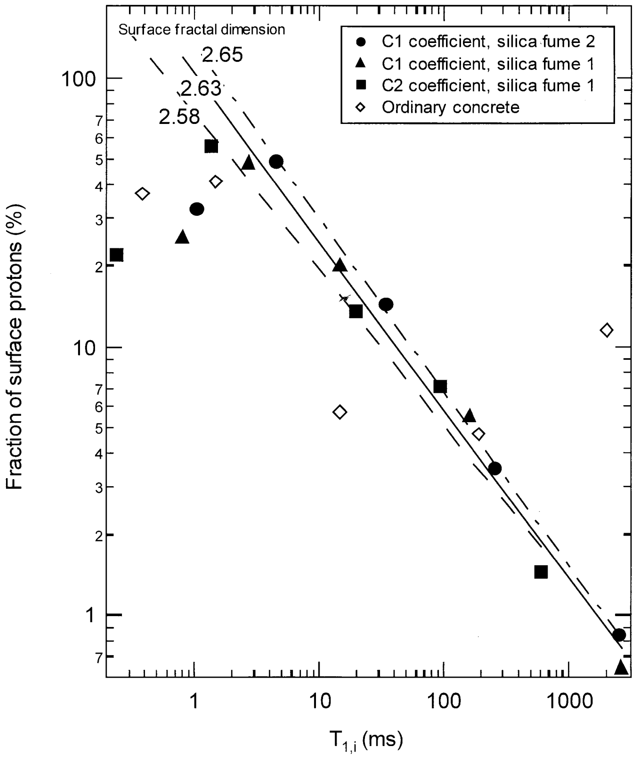

Fig. 2. Logarithmic plot of the fraction of proton magnetization as a function of the relaxation time $T_{1,i}$ for the three reactive powder concrete and ordinary concrete formulations labeled in the text. The dotted lines are the best fits obtained with a power law.

The divergence observed in Fig. 2 confirms that the relaxation process occurs mainly through protons on the surface of nonconnected or badly connected pores, as was previously assumed [2]. The values of D_f, thus derived from the slope of the power law, are displayed for each sample in Fig. 2 and range between 2.58 and 2.65. These results are coherent with previous works [6–8]. We note that D_f is the highest for the formulation with C_1 filling ratio and S_2 silica fume, which has the larger BET surface. D_f is the lowest for the formulation with C_2 filling ratio and the other silica fume S_1. Physically, the more frequent the smallest pores are, the more frequent are the protons relaxing on their surface and the closer to 3 is supposed to be D_f. Thus, the surface fractal dimension is sensitive to the filling ratio and to the specific surface area of silica fume.

On the other hand, the ordinary concrete presents quasi-bimodal porosity features. While the two smaller T_1 are quite similar to the ones observed for reactive powder concrete, the amount of protons in the larger pore range is much more important, as expected in this type of concrete. These results confirm the assessment of the larger T_1 to free water in capillary pores and of the smaller ones to the C-S-H-related porosity. The heterogeneity of the pore size distribution resulting from the presence of coarse aggregates explains the nonobservation of a power law over several orders of magnitude in this type of concrete.

Another indication of the hierarchical nature of the discrete pore distribution in reactive powder concrete is given by the ratio $\alpha = T_{1,i+1}/T_{1,i}$, which is directly linked to the dilatation coefficient between two pore size categories. The measured values of $T_{1,i}$, α, and $P_{1,i}$ are listed in Table 2. Although there are some disparities, α is of the same order of magnitude between two consecutive *i*-values for each formulation. It is all the more obvious for the formulation with C_1 filling ratio and the silica fume S_2. For this formulation, the well-defined α, averaged at around 7.3, is in accordance with an Apollonian packing. This value is also quite close to the dilatation coefficient $\alpha \sim 10.0$ selected by Richard and Cheyrezy [1] for the particle size

Table 2
Distribution of the relaxation times $T_{1,i}$, of the prefactors $P_{1,i}$ and the ratio $\alpha = T_{1,i+1}/T_{1,i}$ for each reactive powder concrete formulation

C_1 coefficient, silica fume S_1 (12 m^2/g BET)			C_2 coefficient, silica fume S_1 (12 m^2/g BET)			C_1 coefficient, silica fume S_2 (21.5 m^2/g BET)		
$T_{1,i}$ (ms)	$P_{1,i}$ (%)	$T_{1,i+1}/T_{1,i}$	$T_{1,i}$ (ms)	$P_{1,i}$ (%)	$T_{1,i+1}/T_{1,i}$	$T_{1,i}$ (ms)	$P_{1,i}$ (%)	$T_{1,i+1}/T_{1,i}$
0.8	25.5	3.4	0.2	22.0	5.7	1.0	32.4	4.3
2.7	48.3	5.4	1.3	56.0	14.6	4.5	48.9	7.6
14.7	20.0	11.0	19.5	13.5	4.8	34.2	14.3	7.6
161.8	5.5	16.3	93.5	7.1	6.4	260.5	3.5	9.8
2645.1	0.7	–	599.9	1.4	–	2551.8	0.9	–
Average $\alpha = T_{1,i+1}/T_{1,i}$		9.0	Average $\alpha = T_{1,i+1}/T_{1,i}$		7.9	Average $\alpha = T_{1,i+1}/T_{1,i}$		7.3
Fractal dimension		2.63	Fractal dimension		2.58	Fractal dimension		2.65

grading of dry components in reactive powder concrete as can be seen in Table 1. Fig. 2 and Table 2 thus clearly show a correlation between the fractal feature of the granular packing and the pore size distribution, since D_f increases for a higher filling ratio, namely, a higher silica fume content, and a larger BET surface of silica fume.

3.2. ^{29}Si NMR results

We have performed ^{29}Si NMR to follow the dependence between the amount of C-S-H and the reactive powder concrete formulation parameters, namely, both the filling ratio and the type of silica fume. This method allows a quantitative observation of the silicon chemical environment in a given material, provided the respect of the relaxation of all silicate species. The ^{29}Si MAS NMR spectra are displayed in Fig. 3. Each peak corresponds to a given chemical environment of silicon nuclei and is assessed according to Engelhardt and Michel [9] chemical shift tables for silicates. In particular, we could sort the cement, which presents Q_0 species at − 71.0 ppm; the C-S-H presenting Q_1 and Q_2 species at − 80.0 and − 84.9 ppm, respectively; the silica fume, sand, and crushed quartz, which presents Q_4 species at − 110.6 and − 107.2 ppm, respectively. The position of the C-S-H peaks is in accordance with previous works [10–12] on synthesized C-S-H. The experimental conditions respect the relaxation times of all species except crushed quartz and sand, which are not chemically reactive at room temperature. This decomposition, as far as the C-S-H and silica fume are concerned, is displayed in Table 3. The relative amount of C-S-H is more important for C_1 filling ratio than for C_2, and is comparable for both silica fumes, with 30% for S_1 and 31% for S_2. These results are not surprising for there is half less initial silica fume in the reactive powder concrete formulation with C_2 filling ratio as can be seen in Table 1, and for silica fume, S_2 has a BET surface almost double that of S_1. Silica fume has indeed the property to enhance the formation of C-S-H by reaction with residual portlandite through the pozzolanic reaction. It also reacts with the C-S-H resulting from the hydration of cement in order to form secondary C-S-H of lower C/S ratio. From the ratio Q_2/Q_1, we obtain information on C-S-H tetrahedra chains, which unsurprisingly appear longer for C_1 than C_2 formulation, and even longer for silica fume S_2 formulation. The average chain length observed for C_2 formulation corresponds to a mixture of mostly pentamers and other shorter chains, resulting in a statistical Q_2/Q_1 of 1.1. In the case of C_1, the at least twice higher Q_2/Q_1 ratio can be interpreted as a mixture of chains containing mostly 10 tetrahedra with the most reactive silica fume. Considering that the hydration of C_3S provides principally dimers in the C-S-H after three months hydration [13], the high values observed for our samples are most likely due to the pozzolanic reaction. We observe a lot of remaining silica fume at the time of the experiment, especially in the formulation with C_1 filling ratio and silica fume S_1. Table 3 thus highlights the higher reactivity of silica fume S_2 compared to S_1: the ratio of the remaining silica fume to all chemically reactive silicate species is more important for silica fume S_1 than for S_2.

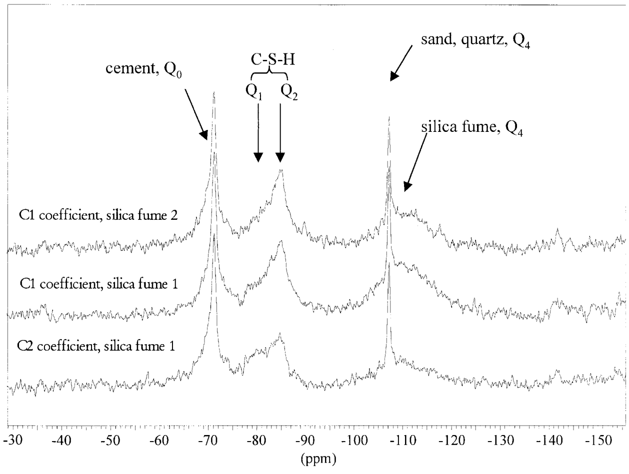

Fig. 3. ^{29}Si MAS NMR spectra of the three reactive powder concrete formulations recorded at 11.7 Tesla (4 mm rotor, 1200 scans) using a spinning speed of 7 kHz and a 30-s delay between two scans in order to have quantitative spectra.

As expected, the amount of C-S-H is more important when there is more silica fume in between the cement grains, which is the case for the formulation with C_1 filling ratio. Obviously, the chain length of C-S-H is also increased by a larger filling ratio, and by a larger BET surface of silica fume, namely S_2. Thus, the amount of C-S-H and their average silicon tetrahedra chain length, deduced from the quantitative decomposition, follow the

Table 3
Relative amounts, expressed in percentage, of C-S-H and silica fume after one month hydration of the three reactive powder concrete formulations, deduced from the fit of the ^{29}Si NMR spectra

Formulation	C_1 coefficient, silica fume 2	C_1 coefficient, silica fume 1	C_2 coefficient, silica fume 1
Relative amount of C-S-H $(Q_1+Q_2)/(Q_0+Q_1+Q_2+Q_{4SF})$	31%	30%	21%
Relative amount of silica fume $Q_{4SF}/(Q_0+Q_1+Q_2+Q_{4SF})$	33%	42%	32%
C-S-H Q_2/Q_1 ratio	3.8	3.0	1.1

They are expressed relatively to all chemically reactive silicate species, Q_{4SF} being the contribution of Q_4 from silica fume. C-S-H Q_2/Q_1 percentage ratio is linear with the average C-S-H chain length.

same dependence as D_f with the reactive powder concrete formulation parameters. They provide a signature of the textural properties of this type of concrete. Protons nuclear magnetic relaxation and ^{29}Si NMR show that the more and the longer C-S-H in the concrete, the larger is the surface on which protons can relax.

4. Conclusions

In this study, the impact of formulation parameters on the texture of concrete was evidenced by using two NMR techniques. The analysis of proton nuclear relaxation inside several one-month-old reactive powder concrete formulations has revealed the reproducible fractal and discrete features of their pore size distribution. It is very likely to be closely related to the almost fractal granular packing of such a type of concrete. We were able to characterize the pore distribution of a reactive powder concrete by only one parameter, namely, the surface fractal dimension. Moreover, the microstructure of concrete was investigated by ^{29}Si NMR experiments and, besides showing the efficiency of one silica fume over another, it provided a feedback of our ^{1}H NMR results. A correlation between the texture of concrete, the length of silicate chains, and the amount of C-S-H was established. ^{1}H and ^{29}Si NMR are expected to be relevant, for instance, in the study of aging or leaching phenomena, which may modify the pore distribution of concrete.

Acknowledgments

The present study has been carried out in the framework of the BRITE EURAM Program BE97-4452 UNICORN, with a financial contribution from the Commission. We also acknowledge the French Ministry of Research for financial support on REACTIF. In particular, we would like to thank Marcel Cheyrezy for the cooperation with Bouygues as well as Christian Vernet. We are also very grateful to Armelle Leboulvais and Fabienne Bégaud who assisted in the casting of concrete samples at Bouygues research laboratories.

References

[1] P. Richard, M. Cheyrezy, Composition of reactive powder concretes, Cem. Concr. Res. 25 (1995) 1501.

[2] J.-P. Korb, D. Petit, S. Philippot, H. Zanni, V. Marret, M. Cheyrezy, Nuclear relaxation of water confined in reactive powder concrete, in: P. Colombet, A.-R. Grimmer, H. Zanni, P. Sozzani (Eds.), Nuclear Magnetic Resonance Spectroscopy of Cement-Based Materials, Springer-Verlag, Berlin, Heidelberg, 1988, pp. 333–343.

[3] S. Philippot, J.-P. Korb, D. Petit, G. Counio, H. Zanni, Analysis of microporosity of reactive powder concrete by proton nuclear relaxation, J. Chim. Phys. 95 (1998) 332–336.

[4] S. Philippot, J.-P. Korb, D. Petit, H. Zanni, Analysis of microporosity and setting of reactive powder concrete by proton nuclear relaxation, Magn. Reson. Imaging 16 (5/6) (1998) 515–519.

[5] S.W. Provencher, A general purpose constrained regularization program for inverting noisy linear algebraic and integral equation, Comput. Phys. Commun. 27 (1982) 229.

[6] V. Baroghel-Bouny, Caractérisation des pâtes de ciment et des bétons, Laboratoire Central des Ponts et Chaussées, Paris, France, 1994.

[7] A.J. Allen, R.C. Oberthur, D. Pearson, P. Schofield, C.R. Wilding, Development of the fine porosity and gel structure of hydrating cement systems, Philos. Mag. B. 56 (3) (1987) 263.

[8] R.G. Blinc, G. Lahajnar, S. Zumer, NMR study of the time evolution of the fractal geometry of cement gels, Phys. Rev. B. 38 (4) (1988) 2873.

[9] G. Engelhardt, D. Michel, High-Resolution Solid-State NMR of Silicates and Zeolites, Wiley, Chichester, 1987.

[10] E. Lippmaa, M. Mägi, M. Tarmak, W. Wieker, A.R. Grimmer, A high resolution ^{29}Si NMR study of the hydration of tricalcium silicate, Cem. Concr. Res. 12 (1982) 597–602.

[11] S.A. Rodger, G.W. Groves, N.J. Clayden, C.M. Dobson, Hydration of tricalcium silicate followed by ^{29}Si NMR with cross-polarization, J. Am. Ceram. Soc. 71 (2) (1988) 91–96.

[12] I. Klur, B. Pollet, J. Virlet, A. Nonat, C-S-H structure evolution with calcium content by multinuclear NMR, in: P. Colombet, A.-R. Grimmer, H. Zanni, P. Sozzani (Eds.), Nuclear Magnetic Resonance Spectroscopy of Cement-Based Materials, Springer-Verlag, Berlin, Heidelberg, 1998, pp. 119–141.

[13] A.R. Brough, C.M. Dobson, I.G. Richardson, G.W. Groves, Application of selective ^{29}Si isotopic enrichment to studies of the structure of calcium silicate hydrate (C-S-H) gels, J. Am. Ceram. Soc. 77 (2) (1994) 593–596.